JCI The Journal of Clinical Investigation

Sex, age, and hospitalization drive antibody responses in a COVID-19 convalescent plasma donor population

Sabra L. Klein, … , Arturo Casadevall, Aaron A. R. Tobian

J Clin Invest. 2020. https://doi.org/10.1172/JCI142004.

Research In-Press Preview COVID-19

Graphical abstract

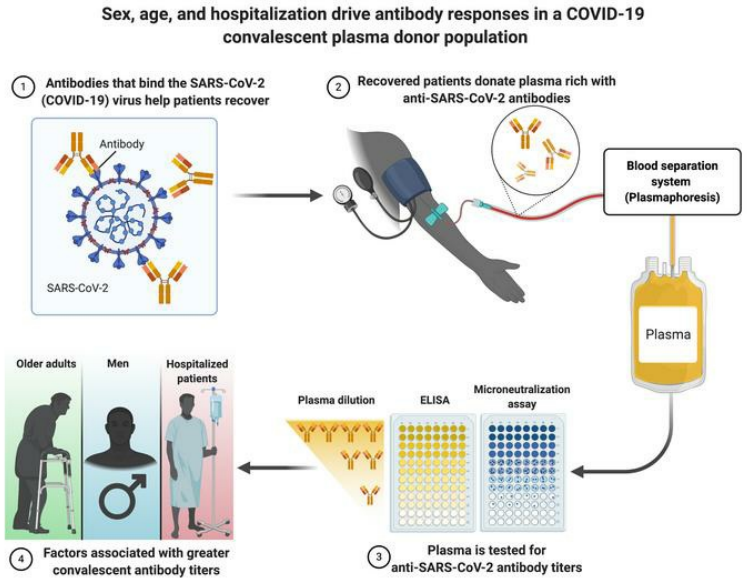

Sex, age, and hospitalization drive antibody responses in a COVID-19 convalescent plasma donor population

Authors: Sabra L. Klein, Ph.D. [1,2,3,*,†], Andrew Pekosz, Ph.D. [1,4] Han-Sol Park, Ph.D. [1], Rebecca L. Ursin, M.S. [2], Janna R. Shapiro, M.S.[3], Sarah E. Benner, Ph.D.,[5] Kirsten Littlefield, B.S. [1], Swetha Kumar, M.S.[6], Harnish Mukesh Naik, M.S.[6], Michael J. Betenbaugh, Ph.D.[6], Ruchee Shrestha M.P.H.[5], Annie A. Wu, B.S.[5], Robert M. Hughes, M.D., Ph.D.[5], Imani Burgess B.A.[5], Patricio Caturegli, M.D. [5], Oliver Laeyendecker, Ph.D.[7,8], Thomas C. Quinn, M.D. [7,8], David Sullivan, M.D. [1], Shmuel Shoham, M.D. [7], Andrew D. Redd, Ph.D. [7,8], Evan M. Bloch, M.D. [5, †], Arturo Casadevall, M.D., Ph.D. [1, †], Aaron A.R. Tobian, M.D., Ph.D. [5, *,†]

Affiliations:
[1] W. Harry Feinstone Department of Molecular Microbiology and Immunology, Johns Hopkins Bloomberg School of Public Health, Baltimore, MD, USA
[2] Department Biochemistry and Molecular Biology, Johns Hopkins Bloomberg School of Public Health, Baltimore, MD, USA
[3] Department of International Health, Johns Hopkins Bloomberg School of Public Health, Baltimore, MD, USA
[4] Department of Environmental Health and Engineering, Johns Hopkins Bloomberg School of Public Health, Baltimore, MD, USA
[5] Department of Pathology, Johns Hopkins School of Medicine, Baltimore, MD, USA
[6]Advanced Mammalian Biomanufacturing Innovation Center, Department of Chemical and Biomolecular Engineering, Johns Hopkins University, Baltimore, MD, USA
[7] Department of Medicine, Division of Infectious Diseases, Johns Hopkins School of Medicine, Baltimore, MD, USA
[8] Division of Intramural Research, National Institute of Allergy and Infectious Diseases, National Institutes of Health, Bethesda, MD, USA

* corresponding authors:
Sabra L. Klein, Ph.D., W. Harry Feinstone Department of Molecular Microbiology and Immunology, Bloomberg School of Public Health, Johns Hopkins University, 615 N. Wolfe St., Baltimore, MD 21205; Email: sklein2@jhu.edu
Aaron A. R. Tobian, M.D., Ph.D., Department of Pathology, School of Medicine, Johns Hopkins University, 600 N. Wolfe St., Carnegie Room 437, Baltimore, MD 21287; Email: atobian1@jhmi.edu

†co-senior authors

Short title: COVID-19 convalescent plasma antibody responses

Conflict of interests: EMB reports personal fees and non-financial support from Terumo BCT, personal fees and non-financial support from Grifols Diagnostics Solutions, outside of the submitted work; EMB is a member of the United States Food and Drug Administration (FDA) Blood Products Advisory Committee. Any views or opinions that are expressed in this manuscript are that of the author's, based on his own scientific expertise and professional judgment; they do not necessarily represent the views of either the Blood Products Advisory Committee or the formal position of FDA, and also do not bind or otherwise obligate or commit either Advisory Committee or the Agency to the views expressed.

Abstract:

Convalescent plasma is a leading treatment for COVID-19, but there is a paucity of data identifying therapeutic efficacy. Among 126 potential convalescent plasma donors, the humoral immune response was evaluated by a SARS-CoV-2 virus neutralization assay using Vero-E6-TMPRSS2 cells, commercial IgG and IgA ELISA to spike (S) protein S1 domain (Euroimmun), IgA, IgG and IgM indirect ELISAs to the full-length S or S-receptor binding domain (S-RBD), and an IgG avidity assay. Multiple linear regression and predictive models were utilized to assess the correlations between antibody responses with demographic and clinical characteristics. IgG titers were greater than either IgM or IgA for S1, full length S, and S-RBD in the overall population. Of the 126 plasma samples, 101 (80%) had detectable neutralizing antibody (nAb) titers. Using nAb titers as the reference, the IgG ELISAs confirmed between 95-98% of the nAb positive, but 20-32% of the nAb negative samples were still IgG ELISA positive. Male sex, older age, and hospitalization with COVID-19 were associated with increased antibody responses across the serological assays. There was substantial heterogeneity in the antibody response among potential convalescent plasma donors, but sex, age, and hospitalization emerged as factors that can be used to identify individuals with a high likelihood of having strong antiviral antibody responses.

Summary: There is substantial heterogeneity in the antibody response to SARS-CoV-2 infection, with greater antibody responses being associated with male sex, advancing age, and hospitalization with COVID-19.

Introduction

Severe acute respiratory syndrome coronavirus 2 (SARS-CoV-2), the causative agent of coronavirus disease 2019 (COVID-19), emerged in Wuhan, China in December 2019. Following the rapid, global spread of SARS-CoV-2, in March 2020, COVID-19 was declared a pandemic. By July 2020, over 17 million cases have been confirmed, spanning 188 countries or territories and accounting for over 660,000 deaths (1). Preventive and treatment options are limited, of which antibody therapy (i.e. convalescent plasma collected from individuals after recovery from COVID-19) has emerged as a leading treatment for COVID-19 (2). Observational findings are encouraging, suggesting improved clinical outcomes in those who are transfused with COVID-19 convalescent plasma (CCP), including radiological resolution, reduction in viral loads, and improved survival (3-8). While two randomized trials assessing CCP China and Europe were terminated early and underpowered, they did not find clinically significant differences between the study arms (6, 9). Nonetheless, there is a lack of standardization of units of CCP that are being transfused, in large part due to limited data correlating antibody assays with formal virus neutralization activity.

Antibody responses that target the immunodominant SARS-CoV-2 spike (S) protein — specifically, those that target the S protein receptor binding domain (S-RBD)— are thought to be highly associated with virus neutralization by blocking the interaction between S-RBD and the virus receptor, angiotensin converting enzyme 2 (AEC2) (10). The SARS-CoV-2 S protein is a highly glycosylated, trimeric protein that requires proteolytic processing to become fusogenic and mediate virus-host membrane fusion (11, 12). The S-RBD domain is partially masked in the pre-fusion structure of S and must be converted to an “open” conformation for optimal binding of S to ACE2 (13). Neutralizing antibodies are of particular interest because they prevent viral

infection by blocking cell surface attachment, as well as inhibiting host membrane fusion (14, 15). Administration of CCP containing these neutralizing antibodies to individuals with COVID-19 has been shown to result in rapid viral clearance, indicating its functionality as an antiviral agent (6). Non-neutralizing antibodies also play a key role in viral clearance as they are needed for antibody dependent cellular cytotoxicity, antibody dependent cell mediated phagocytosis and complement activation (16). The contribution of other antibody types such as IgM and IgA to resolution and potential protection from SARS-CoV-2 infection is not clear. Using plasma samples from 126 recovered COVID-19 patients following mild or moderate disease, we compared a commercial enzyme-linked immunosorbent assay (ELISA), two-step spike protein directed ELISAs, and microneutralization assays, in order to assess how the age and sex of the donor, history of hospitalization for COVID-19, and the time of plasma collection relative to infection could be used to understand the variability of antibody responses to SARS-CoV-2.

Results

Immunoglobulin (Ig) isotyping in COVID-19 convalescent plasma

Convalescent plasma was collected from 126 patients with molecular confirmed SARS-CoV-2 infection. The population consisted of more males (56%) than females, with a median age of 42 years (IQR 29-53) (**Table 1**). Most of the patients were classified as having mild to moderate disease, with <10% having been hospitalized with COVID-19. Plasma samples were collected from patients a median of 43 days (IQR 38-48) after an initial PCR+ nasal swab test. Plasma samples were used for isotyping antibodies that recognized SARS-CoV-2 S antigens. Using the Euroimmun ELISA that recognizes either IgG or IgA against S protein domain S1, we determined that both isotypes were highly detectable in plasma, with arbitrary unit (AU) values

of anti-S1 IgG being greater than IgA ($p<0.05$; **Figure 1A**), but positively associated with each other ($r>0.5$; **Figure 1B**). Consistent results were obtained with the indirect ELISAs that recognized either S or S-RBD, in which titers of IgG, as quantified as area under the curve (AUC), were greater than titers of either IgM or IgA ($p<0.05$ in each case; **Figure 1C** and **1F**). There was considerable heterogeneity in the antibody responses to either S or S-RBD (**Figure 1D** and **1G**), but the AUC values for both anti-S and anti-S-RBD IgG were positively associated with the AUC values for anti-S and anti-S-RBD IgM and IgA, respectively ($r>0.5$ in each case; **Figure 1E** and **1H**). Finally, AUC values for anti-S and anti-S-RBD IgG, IgM, and IgA were strongly correlated with the respective geometric mean titers, with cut-offs set based on the negative control samples run on the same plates (**Figure S1A-O**).

Defining functional antibody in COVID-19 convalescent plasma

To assess the functionality of antibodies that recognize SARS-CoV-2 in convalescent plasma, microneutralization and IgG avidity assays were performed. The reciprocal plasma dilution providing protection from SARS-CoV-2 was used to calculate the AUC for the microneutralization assay. Of the 126 plasma samples screened, 101 (80%) had detectable neutralizing antibodies (nAbs) (**Figure 2A**). The avidity assay defines the binding characteristics of IgG; the OD reading in the presence of various concentrations of urea was used to calculate arbitrary units (AU) for IgG avidity (**Figure 2B**). There was a positive correlation of the results from the microneutralization assay with IgG ELISAs for S1, S, and S-RBD and anti-S1 IgG avidity (**Figure 2C**), with the correlation on nAbs to S-RBD antibodies being strongest and the anti-S1 IgG avidity being weakest. Because virus neutralization is currently considered to be the most critical antibody characteristic associated with potential protection from infection, we

assessed the association of the three S protein IgG ELISAs with the microneutralization assay (**Figure 2D**). We designated cutoffs of >20 for nAbs, < AU 0.8 for S1 IgG, and endpoint titers of <1:320 for S and S-RBD ELISAs. The overall ability of the IgG assays to confirm positive nAb samples was good, with S1-IgG at 96%, S-IgG at 98%, and S-RBD-IgG at 95%. In contrast, the ability of the IgG assays to confirm negative nAb samples was consistently low, with S1-IgG at 32%, S-IgG at 20%, and S-RBD-IgG at 28%. These data suggest that ELISAs may not be superior for confirming samples that do not contain adequate nAb titers.

Host factors contributing to improved antibody responses in COVID-19 convalescent plasma

Using the unadjusted AUC values, we determined that males consistently had greater nAb, anti-S IgG, and anti-RBD IgG than females ($p<0.05$ in each case, **Table S1**). Both nAb and anti-RBD IgG titers, in particular, were consistently higher among males than females within diverse age categories and among non-hospitalized patients (**Table S1** and **Figure S2**).

Multiple linear regression models were used to isolate the effects of sex, age, hospitalization, or time since PCR-positive (PCR+) nasal swab on the antibody response to SARS-CoV-2 while adjusting for the other parameters (**Table S2** and **Figure 3**). As shown in **Figure 3A-P** and **Table S2**, being male, an older adult, and being hospitalized with COVID-19 were each associated with having greater nAb AUC values, anti-S1 IgG AU, anti-S IgG AUC values, and anti-RBD IgG AUC values ($p<0.05$ in each case). When comparing the effect size of each parameter, being hospitalized was associated with the largest increase in antibody response (**Figure 3Q**). Comparing the four assays revealed that being male, older, and hospitalized had the largest effect on the anti-S1-IgG response. The only antibody measure associated with time (days, scaled by 10) since a positive SARS-CoV-2 diagnosis was the nAb response, which was

reduced as the days since the time from the diagnostic PCR+ nasal swab was collected increased (p<0.05; **Figure 3P-Q**).

Predictors of strong antibody responses in donors of COVID-19 convalescent plasma

The convalescent plasma samples were categorized into quartiles based on their nAb AUC value, anti-S1 IgG AU, anti-S IgG AUC value, or anti-RBD IgG AUC value resulting in scores ranging from 0 (lowest quartile for each antibody measure) to 12 (highest quartile for each antibody measure) to model the optimal antibody responses in convalescent plasma (**Figure 4A** and **Table S3**). Thirteen percent (16/126) of donors were in the lowest decile in all measured responses. Multiple linear regression on the composite score encompassing the quartiles for each antibody measure revealed that being male, advancing in age, and hospitalized with severe COVID-19 could each predict greater antibody responses against SARS-CoV-2 (**Figure 4B-D**). In contrast, time elapsed since the diagnostic PCR+ nasal swab was not predictive of greater antibody responses (**Figure 4E**). In terms of effect size, being male resulted in an average numerical increase in score of 1.5 compared to being female, advancing age by a decade resulted in a <1 numerical increase, and being hospitalized resulted in an average increase of 5 in the quartile score (**Figure 4F**). Taken together, these data suggest that being hospitalized with severe COVID-19 and male could be used as predictors of greater convalescent plasma antibody responses against SARS-CoV-2.

Discussion

COVID-19 convalescent plasma has emerged as a leading therapy for hospitalized COVID-19 patients, with thousands of units collected and >30,000 patients treated to date (5,

17). There is a compelling argument for why it could be effective either as prophylaxis after exposure, or as treatment for early disease (17). Consequently, it is important to measure the antibody response following recovery from infection with SARS-CoV-2 responses to understand characteristics for ideal convalescent plasma donation. These data suggest that diverse isotypes of antibody are detectable in plasma approximately 40 days following a positive PCR+ test for SARS-CoV-2, and IgG is the prominent isotype across diverse assays and analyses. Although the commercial ELISA to S1 protein and ELISAs to S and S-RBD correlate well with the positive nAb responses, they were not accurate for confirming samples that were negative for nAb responses. In addition, while overall antibody levels seemed constant, there was a significant decrease in nAbs over time. Overall, greater nAb and IgG titers were associated with male sex, older age, and a history of hospitalization, but further investigation is needed to determine if common or divergent factors are driving these associations.

The heterogeneity in the antibody response demonstrated in this study is consistent with previously published data. While reports from China suggest that the majority of individuals generate greater titers of antibodies ≥14 days after resolution of symptoms (18), 30% of patients do not appear to develop sufficient nAb titers following infection (19). The antibody response induced by coronavirus infection in humans tends to be linked to the severity of the disease. coronaviruses associated with mild disease (e.g., HCoV-229E NL63, OC43 and HKU1) inducing transient levels of antibody, whereas those causing more severe disease (e.g., SARS-CoV and MERS-CoV) inducing stronger and more durable antibody responses (20). Because SARS-CoV-2 infection spans the spectrum of disease, from asymptomatic to lethal, it is not surprising that the induced antibody responses are heterogeneous.

In the present study, 20% of individuals did not have detectable nAbs. Male sex, advancing age, and hospitalization with severe COVID-19 were associated with greater nAb and IgG responses to SARS-CoV-2. Greater IgG titers were correlated with worse COVID-19 outcomes, which is also reflected in the link between greater antibody titers and increased age (21). Male sex also is associated with greater risk of more severe COVID-19 outcomes (22). The greater antibody responses in convalescent plasma from males as compared with females has been reported (23) and is striking given that females usually mount stronger immune responses than males (24). One possible explanation for this apparent reversal in sex-related differences in antibody responses to SARS-CoV-2 is that males with COVID-19 tend to have more severe disease than females, and enhanced inflammatory responses associated with increased disease severity could drive higher B cell recruitment and consequently, more antibody production. In this regard, the magnitude of antibody responses also correlates with disease severity in other infectious diseases, such as active tuberculosis (25).

There are limitations associated with this study. The samples were cross-sectional with a relatively tight window of collection. Therefore, the kinetics of the complete antibody response over time could not be determined, and it was difficult to assess how the time relative to the initial diagnosis correlates with the overall titer. The sampled population, however, represented a clinically diverse population with a wide age range that is representative of the blood donor population. The study was also limited by the lack of measurement of non-direct measures of antibody function (e.g., phagocytosis, antibody-dependent cellular cytotoxicity), but the importance of these mechanisms is not known. Finally, the study focused on antibody responses in plasma, but SARS-CoV-2 antibody responses in the respiratory tract may be critical mediators of protection from infection or severe disease. Understanding the relative contributions of IgG,

IgM, and IgA to SARS-CoV-2 neutralization will provide insights into the nature of protective antibody response (26)

Initially, the FDA recommended that convalescent plasma donors would optimally have ELISA titers exceeding 1:320; this was subsequently lowered given concerns that insufficient donors would attain this threshold (17). Currently, the FDA recommends a NT concentration of $\geq$160, yet allow for a lower titer (1:80) if an alternative is unavailable (27). The FDA, however, has not been prescriptive about the assays used to derive these titer levels despite the potential variability by assay. Data from the Expanded Access Program and clinical trials are urgently needed to interpret the titers with respect to that clinical outcomes and prevention. These results provide a roadmap to select individuals who are likely to have high levels of neutralizing and anti-SARS-CoV-2 IgG antibodies to be preferred convalescent plasma donors.

Methods

Study participants, blood sample processing, and storage

Individuals with a history of COVID-19 who were interested in donating convalescent plasma were contacted by study personnel. All subjects had to be at least 18 years old and have had a confirmed diagnosis of SARS-CoV-2 by detectable RNA on a nasopharyngeal swab. Donors were informed that they needed to satisfy standard eligibility criteria for blood donation (e.g., not pregnant within the last six weeks, never been diagnosed or have risk factors for transfusion-transmitted infections such as HIV, hepatitis B virus or hepatitis C virus). These individuals were then invited to participate in the study. Basic demographic information (age, sex, and hospitalization with COVID-19) was obtained from the subject (i.e. potential donor); confirmation of the original diagnosis of SARS-CoV-2 was required either by medical chart

review or sharing of source documentation, including the date the swab was collected and diagnosis was ascertained. Participants were asked the date of symptom onset, the date the positive swab result was reported, and the date of symptom resolution. Approximately 25 mL of whole blood was collected in ACD tubes. The samples were separated into plasma and peripheral blood mononuclear cells within 12 hours of collection. The plasma samples were immediately frozen at -80^{o}C.

Plasmid preparation

Recombinant plasmid constructs containing modified spike (S) protein or S protein receptor binding domain (RBD) and a beta-lactamase (amp) gene were obtained (28) and amplified in E.coli after transformation and growth on Luria broth (LB) agar plates coated with ampicillin. The plasmids were extracted using GigaPrep kits (Thermo Fisher Scientific) and eluted in molecular biology grade water.

Recombinant protein expression

HEK293.2sus cells (ATCC) were obtained and adapted to Freestyle™ F-17 medium (Thermo Fisher Scientific) and BalanCD® (Irvine Scientific) using polycarbonate shake flasks (Fisherbrand) with 4mM GlutaMAX supplementation (Thermo Fisher Scientific). The cells were routinely maintained every 4 days at a seeding density of 0.5 million cells/mL. They were cultured at 37°C, 90% humidity with 5% CO2 for cells in BalanCD® while those in F-17 were maintained at 8% CO2. Cells were counted using trypan blue dye (Gibco) exclusion method and a haemocytometer. Cell viability was always maintained above 90%. Twenty-four hours prior to transfection (Day -1), the cells were seeded at a density of 1 million cells/mL, ensuring that the cell viability was above 90%. Polyethylenimine (PEI) stocks, with 25 kDa molecular weight

(Polysciences), were prepared in MilliQ water at a concentration of 1 mg/mL. This was sterile filtered through a 0.22 µm syringe filter (Corning), aliquoted and stored at -20°C.

On the day of transfection (Day 0), the cells were counted to ensure sufficient growth and viability. OptiPRO™ SFM (Gibco) was used as the medium for transfection mixture. For 100 mL of cell culture, 2 tubes were aliquoted with 6.7 mL each of OptiPRO™, one for PEI and the other for rDNA. DNA:PEI ratio of 1:3.5 was used for transfection. A volume of 350 µl of prepared PEI stock solution was added to tube 1 while 100 µg of rDNA was added to tube 2 and incubated for 5 minutes. Post incubation, these were mixed together, incubated for 10 minutes at room temperature and then added to the culture through gravity addition. The cells were returned back to the 37°C incubator. A day after transfection (day 1), the cells were spun down at 1,000 rpm for 7 minutes at room temperature and resuspended in fresh media with GlutaMAX™ supplementation. 3-5 hours after resuspension, 0.22 µm sterile filtered Sodium butyrate (EMD Millipore) was added to the flask at a final concentration of 5 mM. The cells were allowed to grow for a period of 4-5 days. Cell counts, viability, glucose and lactate values were measured every day. Cells were harvested when either the viability fell below 60% or when the glucose was depleted, by centrifugation at 5000 rpm for 10 minutes at room temperature. Cell culture supernatants containing either recombinant RBD or S protein were filtered through 0.22 µm polyethersulfone (PES) membrane stericup filters (Millipore Sigma) to remove cell debris and stored at -20°C until purification.

Protein purification

Protein purification by immobilized metal affinity chromatography (IMAC) and gravity flow was adapted from previous methods (28). After washing with phosphate buffered saline (PBS; Thermo Fisher Scientific), Nickel nitrilotriacetic acid (Ni-NTA) agarose (Qiagen) was

added to culture supernatant followed by overnight incubation (12-16 hours) at 4 °C on a rotator. For every 150 mL of culture supernatant, 2.5 mL of Ni-NTA agarose was added. 5mL gravity flow polypropylene columns (Qiagen) were equilibrated with PBS. One polypropylene column was used for every 150 mL of culture supernatant. The supernatant-agarose mixture was then loaded onto the column to retain the agarose beads with recombinant proteins bound to the beads. Each column was then washed, first with 1X culture supernatant volume of PBS and then with 25 mL of 20 mM imidazole (Millipore Sigma) in PBS wash buffer to remove host cell proteins. Recombinant proteins were then eluted from each column in three fractions with 5 mL of 250 mM imidazole in PBS elution buffer per fraction giving a total of 15 mL eluate per column. The eluate was subsequently dialyzed several times against PBS using Amicon Ultra Centrifugal Filters (Millipore Sigma) at 7000 rpm for 20 minutes at 10 °C to remove the imidazole and concentrate the eluate. Filters with a 10 kDa molecular weight cut-off were used for RBD eluate whereas filters with a 50 kDa molecular weight cut-off were used for full length S eluate. The final concentration of the recombinant RBD and S proteins was measured by bicinchoninic acid (BCA) assay (Thermo Fisher Scientific), and purity was assessed on 10% SDS-PAGE (Bio-Rad) followed by Coomassie blue staining. After sufficient destaining in water overnight, clear single bands were visible for RBD and S proteins at their respective molecular sizes.

Viruses and cells

Vero-E6 cells (ATCC CRL-1586) and Vero-E6-TMPRSS2 cells (29) were cultured in Dulbecco's modified Eagle medium (DMEM) containing 10% fetal bovine serum (Gibco), 1 mM glutamine (Invitrogen), 1 mM sodium pyruvate (Invitrogen), 100 U/ml of penicillin

(Invitrogen), and 100 μg/ml of streptomycin (Invitrogen) (complete media or CM). Cells were incubated in a 5% CO2 humidified incubator at 37°C.

The SARS-CoV-2/USA-WA1/2020 virus was obtained from BEI Resources. The infectious virus titer was determined on Vero cells using a 50% tissue culture infectious dose (TCID50) assay as previously described for SARS-CoV (30, 31). Serial 10-fold dilutions of the virus stock were made in infection media (IM; identical to CM except the FBS is reduced to 2.5%), then 100 μl of each dilution was added to Vero cells in a 96-well plate in sextuplicate. The cells were incubated at 37°C for 4 days, visualized by staining with naphthol blue-black, and scored visually for cytopathic effect. A Reed and Muench calculation was used to determine TCID50 per ml (32).

Enzyme-linked Immunosorbent Assays (ELISAs)

Commercial ELISAs and Avidity. The Euroimmun Anti-SARS-CoV-2 ELISA (Mountain Lakes, NJ) for both IgA (cat no. EI2606-9601A) and IgG (cat no. EI2606-9601G) was validated in a Clinical Laboratory Improvement Amendments (CLIA)-certified laboratory. The assay was performed per the manufacturer's specification. The optical density (OD) of the sample divided by the OD of the calibrator from that run, and the ratio is the arbitrary unit (AU). Per the manufacturer, an AU 0-0.79 was considered negative, 0.80-0.99 was borderline and ≥1.0 was positive.

To measure anti-SARS-CoV-2 IgG avidity, each reaction utilized the following components: 100 μl of plasma (1:101 dilution per manufactures protocol), 100 μl of undiluted positive, negative and calibrator controls. Plates containing reaction components were incubated for 1 hour at 37°C followed by 3 washes. A 300 μl volume of wash buffer containing urea at varying concentrations (0M, 1M, 2M, 4M, 6M or 8M) were added to the plates and incubated at

37°C for 10 minutes (33). Plates were washed 3 times, followed by the manufacturer's protocol for addition of conjugate and substrate. Ratios of ≥0.8 were considered positive. DC50 (Dissociation Constant 50) calculations were performed using AAT Bioquest IC50 calculator using four parameter logistic regression model (AAT Bioquest, Inc. (2020, June 09). *Quest Graph™ IC50 Calculator was* retrieved from https://www.aatbio.com/tools/ic50-calculator.

Indirect ELISAs. The protocol was adapted from a published protocol from Dr. Florian Krammer's laboratory (28). Ninety-six well plates (Immulon 4HBX, Thermo Fisher) were coated with either full length S protein or S-RBD at a volume of 50 µl of 2 µg/ml of diluted antigen in filtered, sterile 1xPBS (Thermo Fisher) at 4^{o}C overnight. Coating buffer was removed, plates were washed three times with 300 µl of PBS-T wash buffer (1xPBS plus 0.1% Tween 20, Fisher Scientific), and blocked with 200 µl of PBS-T with 3% non-fat milk (milk powder, American Bio) by volume for one hour at room temperature. All plasma samples were heat inactivated at 56^{o}C on a heating block for one hour prior to use. Negative control samples were prepared at 1:10 dilutions in PBS-T in 1% non-fat milk and plated at a final concentration of 1:100. A monoclonal antibody (mAb) towards the SARS-CoV-2 spike protein was used as a positive control (1:5,000, Sino Biological, Wayne, PA; cat n. 40150-D001). For serial dilutions of plasma on either S or S-RBD-coated plates, plasma samples were prepared in three-fold serial dilutions starting at 1:20 in PBS-T in 1% non-fat-milk. Blocking solution was removed and 10 µl of diluted plasma was added in duplicates to plates and incubated at room temperature for two hours. Plates were washed three times with PBS-T wash buffer and 50 µl secondary antibody was added to plates and incubated at room temperature for one hour. Anti-human secondary antibodies used included Fc-specific total IgG horseradish peroxidase (HRP, 1:5,000 dilution, Invitrogen, cat no. A18823), IgM heavy chain HRP (1:5,000, Invitrogen, cat no. A18835), and

IgA cross-adsorbed HRP (1:5,000, Invitrogen, cat no. A18787); all were prepared in PBS-T plus 1% non-fat milk. Plates were washed and all residual liquid removed before adding 100 µl of SIGMAFAST OPD (o-phenylenediamine dihydrochloride) solution (Sigma Aldrich) to each well, followed by incubation in darkness at room temperature for ten minutes. To stop the reaction, 50 µl of 3M hydrochloric acid (HCl, Fisher Scientific) was added to each well. The OD of each plate was read at 490nm (OD_{490}) on a SpectraMax i3 ELISA plate reader (BioTek). The positive cutoff value for each plate was calculated by summing the average of the negative values and three times the standard deviation of the negatives. All values at or above the cutoff value were considered positive.

Microneutralization assay

Plasma neutralizing antibodies (nAbs) were determined as described for SARS-CoV (34). Two-fold dilutions of plasma (starting at a 1:20 dilution) were made in IM. Infectious virus was added to the plasma dilutions at a final concentration of $1x10^4$ TCID50/ml (100 TCID50 per 100ul). The samples were incubated for one hour at room temperature, then 100 uL of each dilution was added to one well of a 96 well plate of VeroE6-TMPRSS2 cells in sextuplet for 6 hours at 37˚C. The inoculums were removed, fresh IM was added, and the plates were incubated at 37˚C for 2 days. The cells were fixed by the addition of 150 uL of 4% formaldehyde per well, incubated for at least 4 hours at room temperature, then stained with Napthol Blue Black (Sigma-Aldrich). The nAb titer was calculated as the highest serum dilution that eliminated cytopathic effect (CPE) in 50% of the wells.

Statistical analyses

Descriptive analyses. Area under the curve (AUC) values were computed by plotting normalized OD values against sample dilution for ELISAs. AUC for micronentralization assays

utilized the exact number of wells protected from infection at each plasma dilution. For each assay, samples with titers below the limit of detection were assigned an arbitrary AUC value of half of the lowest measured AUC value. The data were then log-transformed to achieve a normal distribution. Descriptive statistics stratified by sex were presented as medians and interquartile ranges, and male-female comparisons overall and in each age category were done using T-tests. A p-value <0.05 was considered statistically significant. AUC values for IgG, IgA, and IgM were compared using a one-way ANOVA. Correlations between antibody isotypes and assays were assessed using Pearson's correlation coefficient. Where binary cut-offs were available, IgG data were dichotomized using the 1:320 cut-off originally recommended by the FDA (17) or the cut-off of AU > 0.8 suggested by the manufacturer. The association between ELISA and microneutralization results were then calculated using nAb titers (i.e. titer > 1:20) as the reference.

Predictors of assay-specific responses. Multiple linear regression models were performed to assess the impact of the demographic (age in decades and sex) and clinical factors (hospitalization status and days since collection of PCR+ swab scaled by 10) on S1-IgG OD values, log AUC values for anti-RBD and anti-spike IgG, as well as nAb. The four time-related terms collected from the participants (i.e., date of symptom onset, date PCR+ swab was collected, date the positive swab result was reported, and date of symptom resolution) were correlated with each other. To avoid collinearity, only the number of days since collection of PCR+ swab was included in analyses, as this was the only metric that was not subject to response and recall bias, and therefore deemed the most reliable. All predictor estimates were adjusted for the three other parameters in the model. Various additional parameters were tested, including and interaction term between age and sex and linear splines at different ages, but

decreased the overall fit of the model and were therefore not included in further analysis. Data are presented as the marginal effect of each predictor for the average person in the study population (35) along with coefficients and 95% confidence intervals of each estimate .

Composite score representing overall quality of antibody response. Composite scores were computed to provide a single metric as a proxy for the overall quality of the antibody response. The responses for S1-IgG, S-IgG, S-RBD and neutralizing assays were divided into quartiles, and subjects were assigned a score of 0 (lowest quartile) to 3 (highest) quartile for each assay. The assay-specific scores were summed to create the composite score, ranging from 0 (lowest quartile for each assay) to 12 (highest quartile for each assay). A multiple linear regression model was then performed on the composite score, including parameters for sex, age in decades, hospitalization status and number of days since collection of PCR+ swab (scaled by ten). As above, data are presented as the marginal effect of each predictor for the average person in the study population (35) along with coefficients and 95% confidence intervals of each estimate. All analyses were performed using GraphPad Prism 8 and Stata 15.

Study approval

The Johns Hopkins University School of Medicine Institutional Review Board reviewed and approved the sample collection and overall study. All participating subjects signed a written informed consent.

Author contributions: E.M.B., A.C., and A.T. conceived and designed the study; E.M.B., D.S., S.S., and A.T. wrote the IRB protocol; R.S., A.W, R.M.H., I.B., E.M.B. and A.T recruited participants; S.L.K., A.P., H-S.P., R.L.U., K.L., O.L., T.Q. S.E.B., A.D.R., P.C., E.M.B, and A.T. carried out all experiments; H.M.N., S.K. and M.J.B. produced recombinant SARS-CoV-2 proteins; J.R.S. performed statistical analyses; S.L.K., A.P.,H-S.P., R.L.U., J.R.S., E.M.B., A.C., and A.T. wrote the manuscript with substantial input from all co-authors.

Acknowledgments: We are grateful for all of the study participants who donated plasma, the clinical staff, including Sonali Thapa and Liz Martinez, Mary De'Jarnette, Carlos Aguado, Peggy Iraola, Jackie Lobien who collected samples, and the technical staff, including Yolanda Eby, Rey Fernandez, Haley Schmidt, Charles Kirby, Ethan Klock, Owen Baker, Jernelle Miller, and Morgan Keruly who aliquoted and stored samples for this study. We thank Florian Krammer of the Icahn School of Medicine at Mount Sinai for providing protocols, plasmids, and initial stocks of ELISA antigens and Daniel Smith for assistance with the graphical abstract generated in Biorender.

Funding This work was supported in part by NIH Specialized Center of Research Excellence U54AG062333 (S.L.K, A.P., H-S.P, J.S.); NIH Center of Excellence in Influenza Research and Surveillance HHSN272201400007C (A.P., K.L., S.L.K., R.L.U.); T32A1007417 Molecular and Cellular Basis of Infectious Diseases (R.L.U.); National Institute of Allergy and Infectious Diseases (NIAID) AI052733 and AI15207 (A.C.); NIAID R01AI120938, R01AI120938S1 and R01AI128779 (A.A.R.T); the Division of Intramural Research, NIAID (O.L., T.Q.); National Heart Lung and Blood Institute 1K23HL151826-01 (E.B.M) and R01HL059842 (A.C.). Bloomberg Philanthropies (A.C.); Department of Defense W911QY2090012 (A.C. and D.S.).

Data and materials availability: All data are contained in the manuscript.

References:

1. JHU. Johns Hopkins University Coronavirus Resource Center. Accessed 7/31/2020, 2020.
2. Casadevall A, and Pirofski LA. The convalescent sera option for containing COVID-19. *J Clin Invest.* 2020.
3. Shen C, Wang Z, Zhao F, Yang Y, Li J, Yuan J, et al. Treatment of 5 Critically Ill Patients With COVID-19 With Convalescent Plasma. *JAMA.* 2020.
4. Duan K, Liu B, Li C, Zhang H, Yu T, Qu J, et al. Effectiveness of convalescent plasma therapy in severe COVID-19 patients. *Proc Natl Acad Sci U S A.* 2020;117(17):9490-6.
5. Joyner MJ, Wright RS, Fairweather D, Senefeld JW, Bruno KA, Klassen SA, et al. Early safety indicators of COVID-19 convalescent plasma in 5,000 patients. *J Clin Invest.* 2020.
6. Li L, Zhang W, Hu Y, Tong X, Zheng S, Yang J, et al. Effect of Convalescent Plasma Therapy on Time to Clinical Improvement in Patients With Severe and Life-threatening COVID-19: A Randomized Clinical Trial. *JAMA.* 2020.
7. Liu STH, Lin H-M, Baine I, Wajnberg A, Gumprecht JP, Rahman F, et al. Convalescent plasma treatment of severe COVID-19: A matched control study. *medRxiv.* 2020:2020.05.20.20102236.
8. Hegerova L, Gooley T, Sweerus KA, Maree CL, Bailey N, Bailey M, et al. Use of Convalescent Plasma in Hospitalized Patients with Covid-19 - Case Series. *Blood.* 2020.
9. Gharbharan A, Jordans CCE, GeurtsvanKessel C, den Hollander JG, Karim F, Mollema FPN, et al. Convalescent Plasma for COVID-19. A randomized clinical trial. *medRxiv.* 2020:2020.07.01.20139857.
10. Zost SJ, Gilchuk P, Case JB, Binshtein E, Chen RE, Reidy JX, et al. Potently neutralizing human antibodies that block SARS-CoV-2 receptor binding and protect animals. *bioRxiv.* 2020.
11. Walls AC, Park YJ, Tortorici MA, Wall A, McGuire AT, and Veesler D. Structure, Function, and Antigenicity of the SARS-CoV-2 Spike Glycoprotein. *Cell.* 2020;181(2):281-92 e6.
12. Wang Q, Zhang Y, Wu L, Niu S, Song C, Zhang Z, et al. Structural and Functional Basis of SARS-CoV-2 Entry by Using Human ACE2. *Cell.* 2020;181(4):894-904 e9.
13. Shang J, Wan Y, Luo C, Ye G, Geng Q, Auerbach A, et al. Cell entry mechanisms of SARS-CoV-2. *Proc Natl Acad Sci U S A.* 2020;117(21):11727-34.
14. VanBlargan LA, Goo L, and Pierson TC. Deconstructing the Antiviral Neutralizing-Antibody Response: Implications for Vaccine Development and Immunity. *Microbiol Mol Biol Rev.* 2016;80(4):989-1010.
15. Klasse PJ. Neutralization of Virus Infectivity by Antibodies: Old Problems in New Perspectives. *Adv Biol.* 2014;2014.
16. Vanderven HA, and Kent SJ. The protective potential of Fc-mediated antibody functions against influenza virus and other viral pathogens. *Immunol Cell Biol.* 2020;98(4):253-63.
17. Bloch EM, Shoham S, Casadevall A, Sachais BS, Shaz B, Winters JL, et al. Deployment of convalescent plasma for the prevention and treatment of COVID-19. *J Clin Invest.* 2020.
18. Duan K, Liu B, Li C, Zhang H, Yu T, Qu J, et al. The feasibility of convalescent plasma therapy in severe COVID-19 patients: a pilot study. *medRxiv.* 2020:2020.03.16.20036145.
19. Wang X, Guo X, Xin Q, Pan Y, Li J, Chu Y, et al. Neutralizing Antibodies Responses to SARS-CoV-2 in COVID-19 Inpatients and Convalescent Patients. *medRxiv.* 2020:2020.04.15.20065623.
20. Sariol A, and Perlman S. Lessons for COVID-19 Immunity from Other Coronavirus Infections. *Immunity.* 2020.
21. Zhang B, Zhou X, Zhu C, Feng F, Qiu Y, Feng J, et al. Immune phenotyping based on neutrophil-to-lymphocyte ratio and IgG predicts disease severity and outcome for patients with COVID-19. *medRxiv.* 2020:2020.03.12.20035048.
22. Scully EP, Haverfield J, Ursin RL, Tannenbaum C, and Klein SL. Considering how biological sex impacts immune responses and COVID-19 outcomes. *Nat Rev Immunol.* 2020.
23. Robbiani DF, Gaebler C, Muecksch F, Lorenzi JCC, Wang Z, Cho A, et al. Convergent antibody responses to SARS-CoV-2 in convalescent individuals. *Nature.* 2020.
24. Flanagan KL, Fink AL, Plebanski M, and Klein SL. Sex and Gender Differences in the Outcomes of Vaccination over the Life Course. *Annu Rev Cell Dev Biol.* 2017;33:577-99.
25. Yu X, Prados-Rosales R, Jenny-Avital ER, Sosa K, Casadevall A, and Achkar JM. Comparative evaluation of profiles of antibodies to mycobacterial capsular polysaccharides in tuberculosis patients and controls stratified by HIV status. *Clin Vaccine Immunol.* 2012;19(2):198-208.
26. Sterlin D, Mathian A, Miyara M, Mohr A, Anna F, Claer L, et al. IgA dominates the early neutralizing antibody response to SARS-CoV-2. *medRxiv.* 2020:2020.06.10.20126532.

27. FDA. Recommendations for Investigational COVID-19 Convalescent Plasma. https://www.fda.gov/vaccines-blood-biologics/investigational-new-drug-ind-or-device-exemption-ide-process-cber/recommendations-investigational-covid-19-convalescent-plasma. Updated 05/01/2020 Accessed 06/18/2020, 2020.
28. Stadlbauer D, Amanat F, Chromikova V, Jiang K, Strohmeier S, Arunkumar GA, et al. SARS-CoV-2 Seroconversion in Humans: A Detailed Protocol for a Serological Assay, Antigen Production, and Test Setup. *Curr Protoc Microbiol.* 2020;57(1):e100.
29. Matsuyama S, Nao N, Shirato K, Kawase M, Saito S, Takayama I, et al. Enhanced isolation of SARS-CoV-2 by TMPRSS2-expressing cells. *Proc Natl Acad Sci U S A.* 2020;117(13):7001-3.
30. Schaecher SR, Touchette E, Schriewer J, Buller RM, and Pekosz A. Severe acute respiratory syndrome coronavirus gene 7 products contribute to virus-induced apoptosis. *J Virol.* 2007;81(20):11054-68.
31. Schaecher SR, Mackenzie JM, and Pekosz A. The ORF7b protein of severe acute respiratory syndrome coronavirus (SARS-CoV) is expressed in virus-infected cells and incorporated into SARS-CoV particles. *J Virol.* 2007;81(2):718-31.
32. Reed LJ, and Meunch H. A simple method of estimating 50 percent endpoints. *American Journal of Hygiene.* 1938;27(3):493.
33. Wang Q, Du Q, Guo B, Mu D, Lu X, Ma Q, et al. A Method To Prevent SARS-CoV-2 IgM False Positives in Gold Immunochromatography and Enzyme-Linked Immunosorbent Assays. *J Clin Microbiol.* 2020;58(6).
34. Schaecher SR, Stabenow J, Oberle C, Schriewer J, Buller RM, Sagartz JE, et al. An immunosuppressed Syrian golden hamster model for SARS-CoV infection. *Virology.* 2008;380(2):312-21.
35. Williams R. Using the margins command to estimate and interpret adjusted predictions and marginal effects. *The Stata Journal.* 2012;12(2):308-31.

Figure 1: IgG is the primary isotype produced against SARS-CoV-2 spike (S) protein. Convalescent plasma samples from recovered COVID-19 patients were used to assess antibody isotypes that recognize SARS-CoV-2 antigens. Commercial kits from Euroimmun were used to measure total IgG and IgA antibodies against the SARS-CoV-2 spike (S) protein domain S1 at an optical density of 450nm (OD450) and were compared to a calibrator to yield arbitrary units (AU) (**A**). The correlation between anti-S1 isotypes is graphed, with the r value noted (**B**). Indirect ELISAs were used to measure IgG, IgM, and IgA antibody levels against S (**C**) and IgG, IgM, and IgA against the S-receptor binding domain (RBD) (**F**) and are graphed as area under the curve (AUC) values. The heterogeneity of the IgG, IgM, and IgA antibody responses against S (**D**) and S-RBD (**G**) are shown in 3D scatter plots, with IgA on the x-axis, IgM on the y-axis, and IgG on the z-axis. The correlations between IgG, IgM, and IgA for S (**E**) and S-RBD (**H**) are included, with *r* values shown and are shaded darker for higher correlation values or lighter for lower correlation values. Graphs show mean + SEM. (n = 126) *$p < 0.05$ (paired t-test).

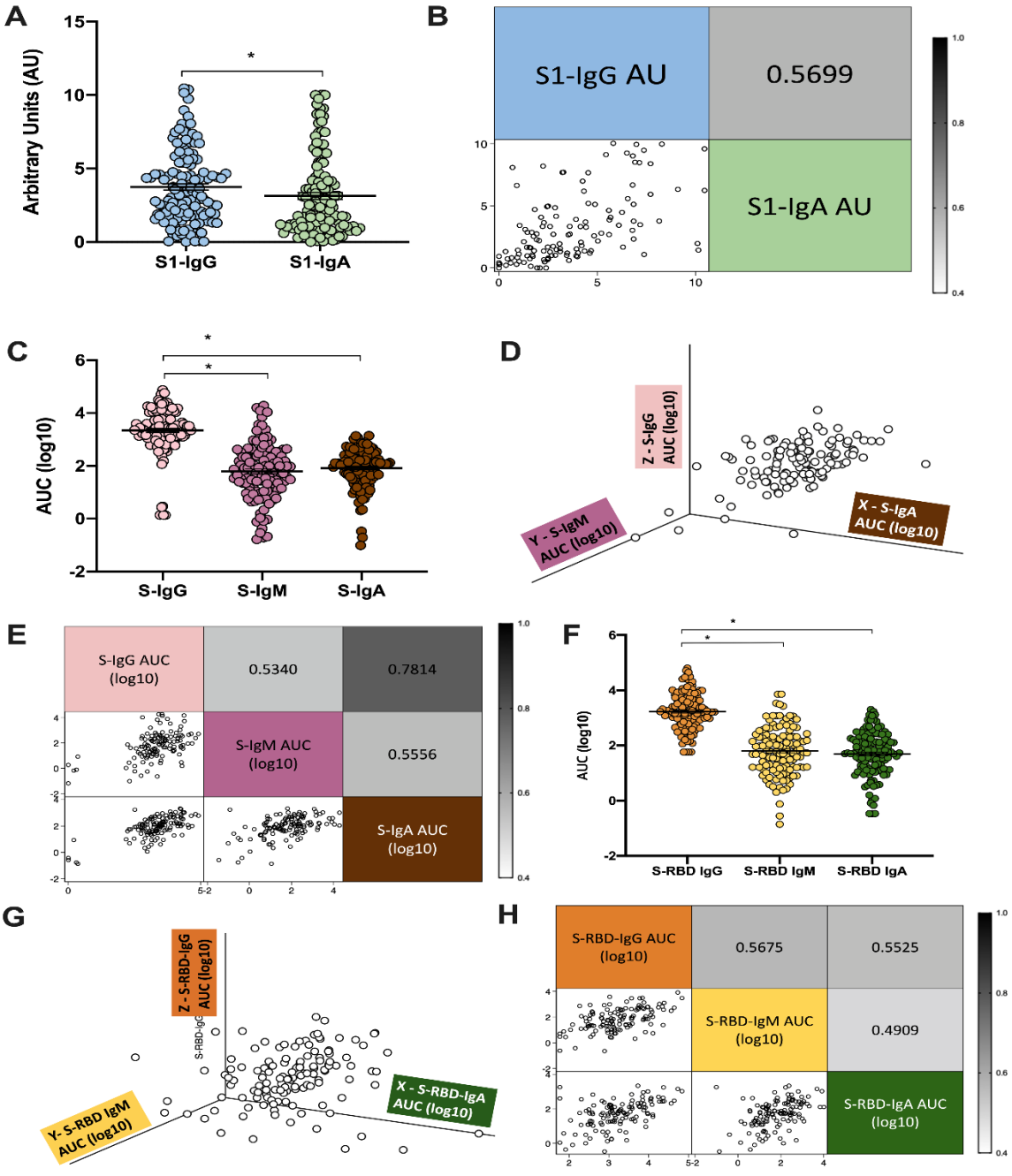

Figure 2: Neutralizing antibody (nAb) titers correlate with IgG antibodies that recognize SARS-CoV-2 spike (S) protein. Convalescent plasma samples from recovered COVID-19 patients were used to assess functional antibody levels. Microneutralization assays were performed on each plasma sample in two-fold serial dilutions, with the area under the curve (AUC) calculated for all samples with titer ≥20 (**A**). Avidity assay used varying amounts of urea to dissociate the anti-S1 spike protein domain IgG/antigen complex from each plasma sample (represented as arbitrary units, AU) to identify the optimal avidity AU ratio (2M urea) for subsequent analyses (**B**). The correlation between nAb AUC values, anti-S1 IgG avidity AU, anti-S1-IgG AU, anti-S-IgG AUC, and anti-S-receptor binding domain (S-RBD)-IgG AUC are shown, with the r values indicated and shaded darker for higher correlation values or lighter for lower correlation values (**C**). For each assay the percentage (%) of positive and negative samples were defined and compared to the nAb AUC, with the negative cutoff value, the number of plasma samples considered positive and negative, as well as how well the ELISAs confirmed the microneutralization assay results, which were the reference (ref) (**D**).

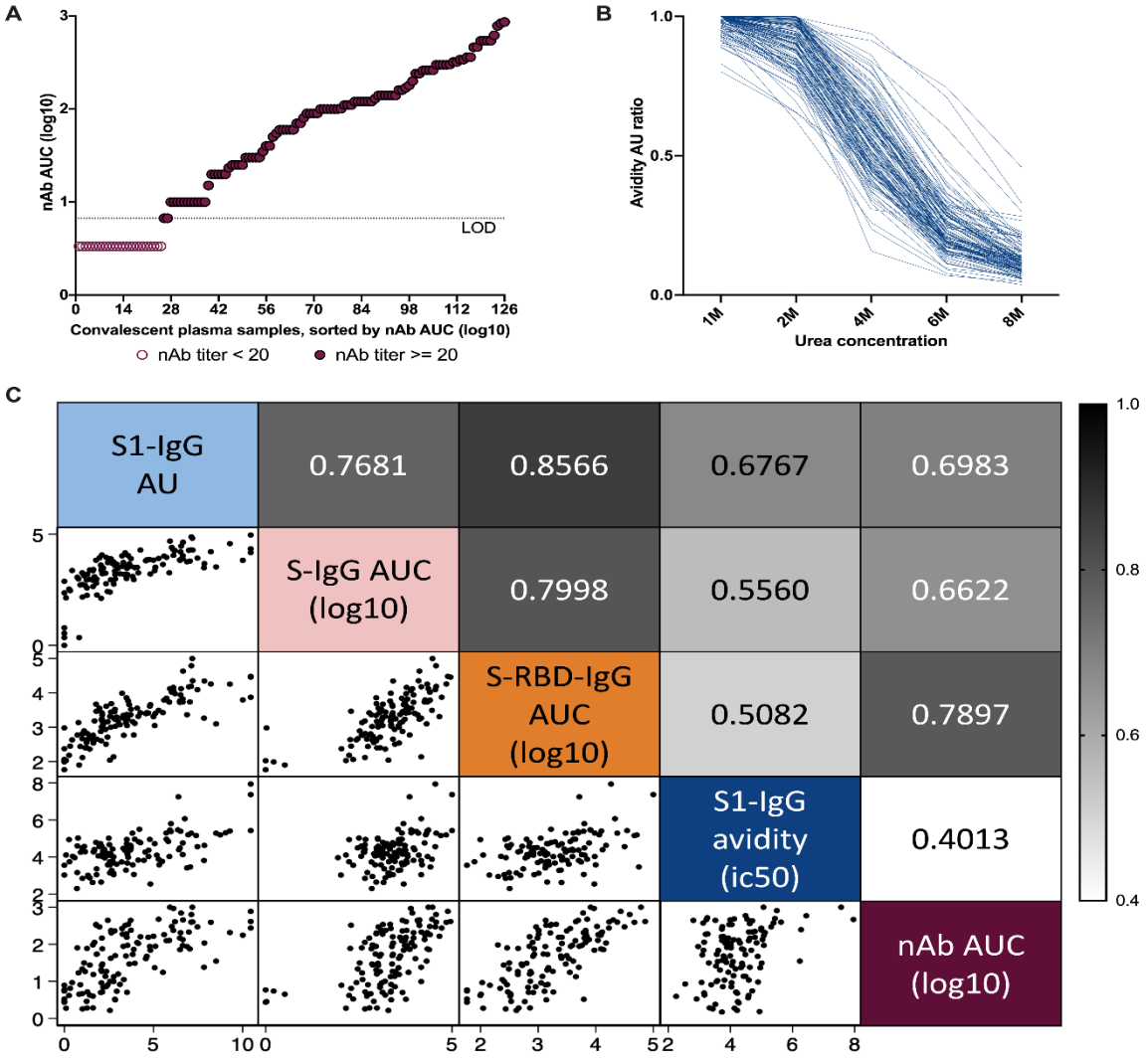

D

Test	Positive	% positive*	Negative	% negative**
nAb titer binary (neg <20)	101	ref	25	ref
S1-IgG (neg < AU 0.8)	114	96	12	32
S-IgG titer (neg < titer 1:320)	119	98	7	20
S-RBD-IgG (neg < titer 1:320)	114	95	12	28

* Percent of samples that had positive nAb titers that were also positive by ELISA

** Percent of samples that had negative nAb titers that were also negative by ELISA

Figure 3: Sex, age, hospitalization, and time since collection of PCR+ nasal swab are associated with antibody responses to SARS-CoV-2. Multiple linear regression models were performed on the continuous outcomes of anti-spike (S) protein domain S1 IgG arbitrary units (AU) (**A**, **E**, **I**, **M**), anti-S-IgG area under the curve (AUC) (**B**, **F**, **J**, **N**), anti-S-RBD AUC (**C**, **J**, **K**, **O**), and neutralizing antibody (NT) AUC (**D**, **H**, **L**, **P**). For each outcome, the model included parameters for the four predictors of interest: sex (**A-D**), age in decades (**E-H**), hospitalization status (**J-L**), and number of days since collection of PCR+ nasal swab (**M-P**). Regression models included the 124 subjects for which complete predictor data was available (hospitalization status was missing for 2 subjects). In each panel, colored circles show the raw data, and white dots show the marginal effect of the given predictor, or the model-predicted outcome (with 95% CI) for the average person for different levels of the given predictor. P-values on top of each panel represent the significance level for the parameter. The four models are summarized in **Q**, where the position of the marker indicates the coefficient value + 95% CI, and stars indicate significance (* = p<0.05).

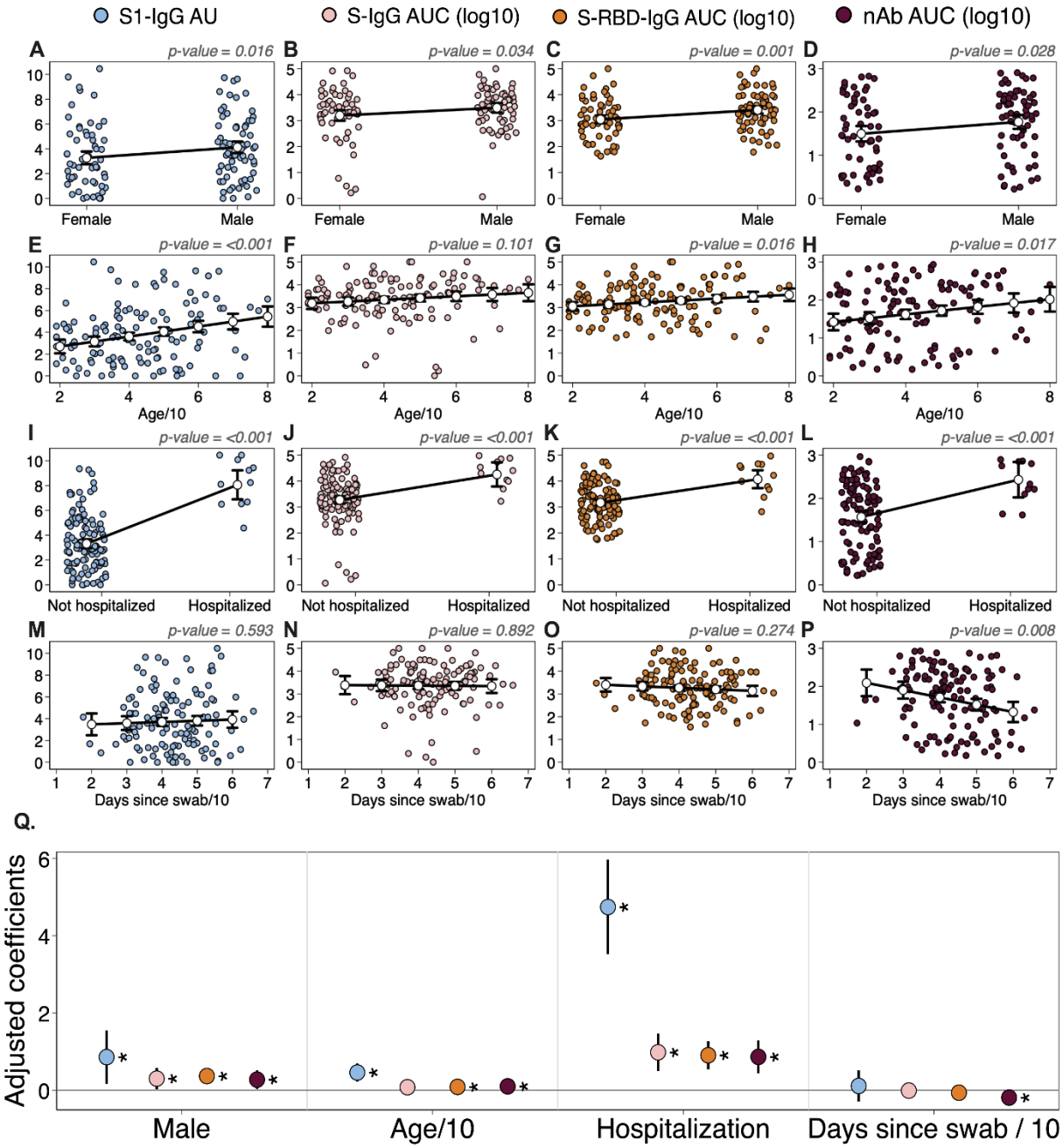

Figure 4: Male sex and hospitalization are predictors of overall greater antibody titers in convalescent plasma. Composite scores were computed for each subject based on the quartile of their response across the anti-spike (S) protein domain S1 IgG, anti-S-IgG, anti-S-receptor binding domain (S-RBD) IgG, and neutralizing antibody (NT) assays (**A**). The distribution of scores among the study population is shown to the right of the heatmap. Multiple linear regression was performed on the continuous outcome of score, including parameters for sex, age in decades, hospitalization status, and number of days since collection of PCR+ nasal swab scaled by ten. For each predictor, the raw data is shown in gray, and the marginal effect + 95% CI of the given predictor for the average individual in the study is shown in white (**B-E**). P-values on top of each panel represent the significance level for the parameter. The model is summarized in **F**, where the position of the marker indicates the coefficient value + 95% CI, or the expected increase in score for a one unit increase in each predictor.

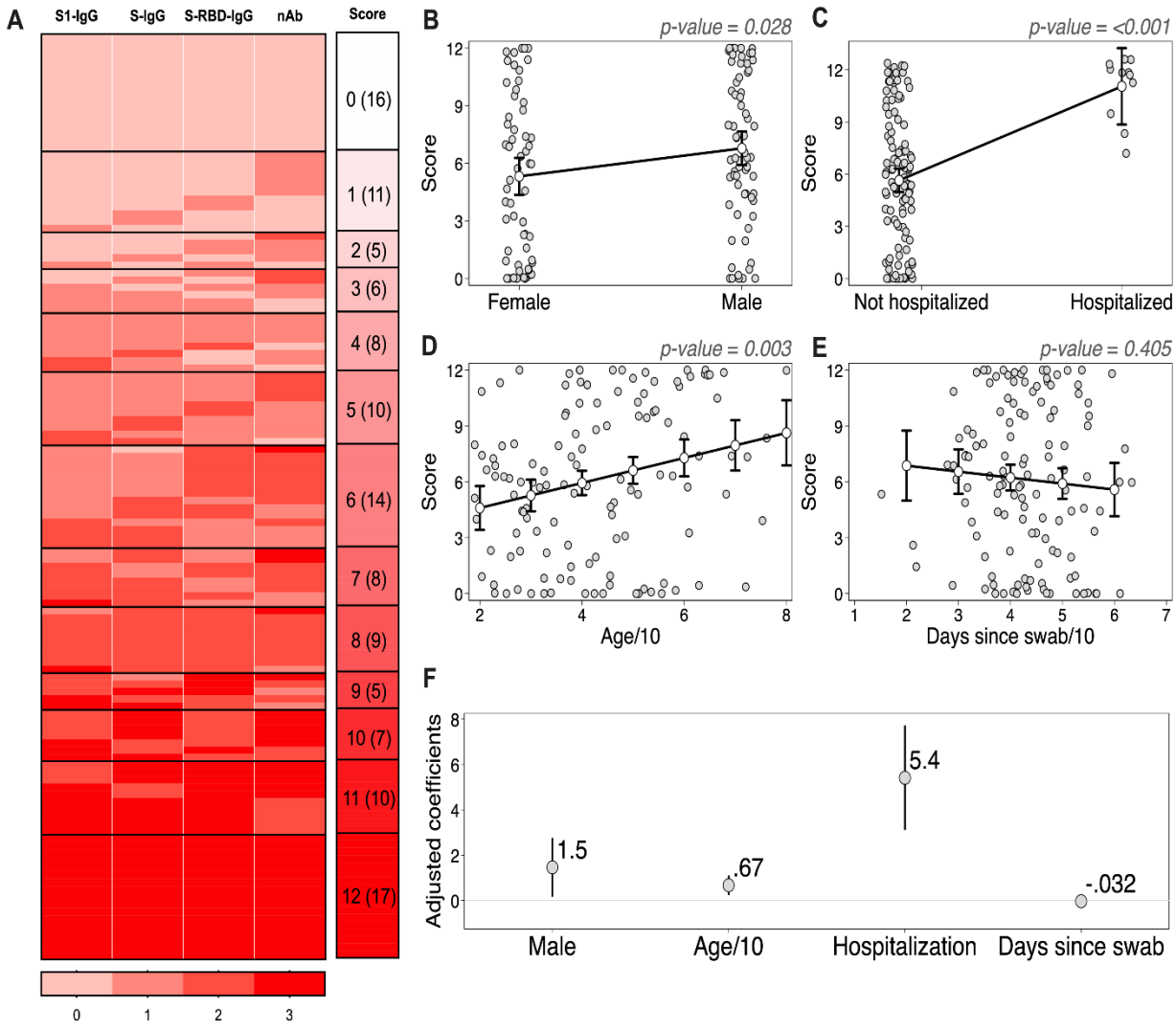

586 **Table 1.** Demographic data from convalescent plasma donors.

587

	All	Females	Males
N (%)	126	58 (46)	68 (54)
Age - med (IQR)	42 (29 - 53)	41.5 (28 - 55)	42 (31.5 - 53)
Age Categories - n (%)			
19-44	74 (58.7)	34 (58.6)	40 (58.8)
45-64	41 (32.5)	19 (32.8)	22 (32.4)
65+	11 (8.7)	5 (8.6)	6 (8.8)
Race/ethnicity - n (%)			
White	94 (74.6)	42 (72.4)	52 (76.5)
African American	4 (3.2)	1 (1.7)	3 (4.4)
Asian	14 (11.1)	8 (13.8)	6 (8.8)
Hispanic	5 (4)	2 (3.4)	3 (4.4)
Mixed/other/unknown	9 (7.1)	5 (8.6)	4 (5.9)
Hospitalized - n (%)[a]	11 (8.9)	6 (10.7)	5 (7.4)
No of days - med (IQR)	5 (2-6)	5 (2-5)	4 (3-6)
Days since swab collection - med (IQR)	43 (38-48)	44.5 (39-49)	41 (37-48)

[a] Hospitalization status missing for 2 donors. Percentages calculated out of total of available data.

588